DC–AC Cascaded H-Bridge Multilevel Boost Inverter With No Inductors for Electric/Hybrid Electric Vehicle Applications

Zhong Du, *Member, IEEE*, Burak Ozpineci, *Senior Member, IEEE*,
Leon M. Tolbert, *Senior Member, IEEE*, and John N. Chiasson, *Senior Member, IEEE*

***Abstract*—This paper presents a cascaded H-bridge multilevel boost inverter for electric vehicle (EV) and hybrid EV (HEV) applications implemented without the use of inductors. Currently available power inverter systems for HEVs use a dc–dc boost converter to boost the battery voltage for a traditional three-phase inverter. The present HEV traction drive inverters have low power density, are expensive, and have low efficiency because they need a bulky inductor. A cascaded H-bridge multilevel boost inverter design for EV and HEV applications implemented without the use of inductors is proposed in this paper. Traditionally, each H-bridge needs a dc power supply. The proposed design uses a standard three-leg inverter (one leg for each phase) and an H-bridge in series with each inverter leg which uses a capacitor as the dc power source. A fundamental switching scheme is used to do modulation control and to produce a five-level phase voltage. Experiments show that the proposed dc–ac cascaded H-bridge multilevel boost inverter can output a boosted ac voltage without the use of inductors.**

***Index Terms*—Cascaded H-bridge multilevel boost inverter, electric vehicle (EV)/hybrid electric vehicle (HEV).**

I. Introduction

RECENTLY, because of increasing oil prices and environmental concerns, hybrid electric vehicles (HEVs) and electric vehicles (EVs) are gaining increased attention due to their higher efficiencies and lower emissions associated with the development of improved power electronics [1]–[3] and motor technologies [4]–[9]. An HEV typically combines a smaller internal combustion engine of a conventional vehicle with a battery pack and an electric motor to drive the vehicle. The combination offers lower emissions but with the power range and convenient fueling of conventional (gasoline and diesel) vehicles. An EV typically uses rechargeable batteries and an electric motor. The batteries need to be charged regularly.

Both HEVs and EVs need a traction motor and a power inverter to drive the traction motor. The requirements for the power inverter include high peak power and low continuous power rating. Currently available power inverter systems for HEVs use a dc–dc boost converter to boost the battery voltage for a traditional three-phase inverter. If the motor is running at low to medium power, the dc–dc boost converter is not needed, and the battery voltage will be directly applied to the inverter to drive the traction motor. If the motor is running in a high power mode, the dc–dc boost converter will boost the battery voltage to a higher voltage, so that the inverter can provide higher power to the motor. Present HEV traction drive inverters have low power density, are expensive, and have low efficiency because they need bulky inductors for the dc–dc boost converters. To achieve a boosted output ac voltage from the traditional inverters for HEV and EV applications, the Z-source inverter is proposed, which also requires an inductor [10].

A cascaded H-bridge multilevel boost inverter shown in Fig. 1 for EV and HEV applications is described in this paper. Traditionally, each H-bridge of a cascaded multilevel inverter needs a dc power supply [4]–[6]. The proposed cascaded H-bridge multilevel boost inverter uses a standard three-leg inverter (one leg for each phase) and an H-bridge in series with each inverter leg which uses a capacitor as the dc power source [11]–[14]. In this topology, the need for large inductors is eliminated. A fundamental switching scheme is used to do modulation control and to output five-level phase voltages. Experiments show that the proposed dc–ac cascaded H-bridge multilevel boost inverter without inductors can output a boosted ac voltage.

II. Working Principle of Cascaded H-Bridge Multilevel Boost Inverter Without Inductors

The topology of the proposed dc–ac cascaded H-bridge multilevel boost inverter is shown in Fig. 1. The inverter uses a standard three-leg inverter (one leg for each phase) and an H-bridge with a capacitor as its dc source in series with each phase leg.

Paper IPCSD-08-070, presented at the 2007 Industry Applications Society Annual Meeting, New Orleans, LA, September 23–27, and approved for publication in the IEEE TRANSACTIONS ON INDUSTRY APPLICATIONS by the Industrial Power Converter Committee of the IEEE Industry Applications Society. Manuscript submitted for review January 6, 2008 and released for publication September 30, 2008. Current version published May 20, 2009. This work was supported by the Oak Ridge National Laboratory, Oak Ridge, TN, which is managed by UT-Battelle for the U.S. Department of Energy under Contract DE-AC05-00OR22725.

Z. Du was with Oak Ridge National Laboratory, Knoxville, TN 37932 USA. He is now with Parker Hannifin Corporation, Olive Branch, MS 38654 USA (e-mail: zhong.du@parker.com).

B. Ozpineci is with the Power Electronics and Electric Machinery Research Center, Oak Ridge National Laboratory, Knoxville, TN 37932 USA (e-mail: ozpinecib@ornl.gov).

L. M. Tolbert is with the Department of Electrical Engineering and Computer Science, The University of Tennessee, Knoxville, TN 37996 USA, and also with the Oak Ridge National Laboratory, Knoxville, TN 37932 USA (e-mail: tolbert@utk.edu).

J. N. Chiasson is with Boise State University, Boise, ID 83725 USA (e-mail: JohnChiasson@boisestate.edu).

Color versions of one or more of the figures in this paper are available online at http://ieeexplore.ieee.org.

Digital Object Identifier 10.1109/TIA.2009.2018978

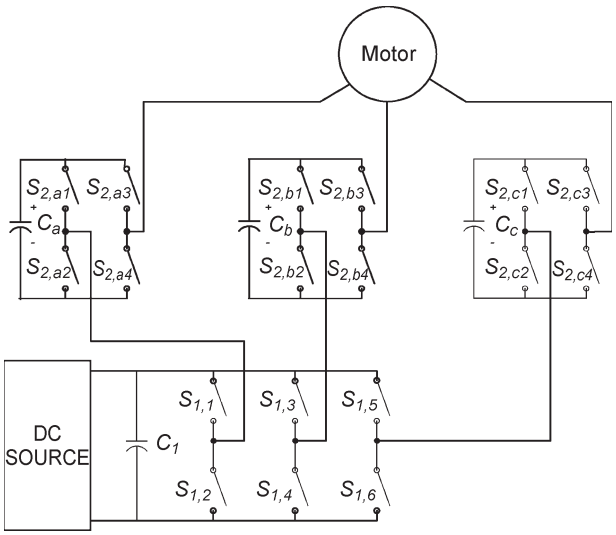

Fig. 1. Topology of the proposed dc–ac cascaded H-bridge multilevel boost inverter.

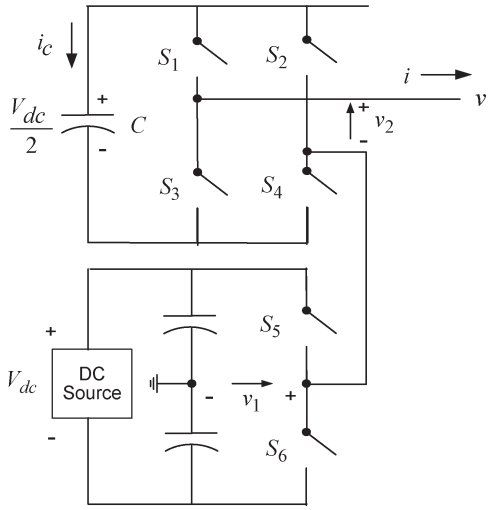

Fig. 2. Single phase of the proposed dc–ac cascaded H-bridge multilevel boost inverter.

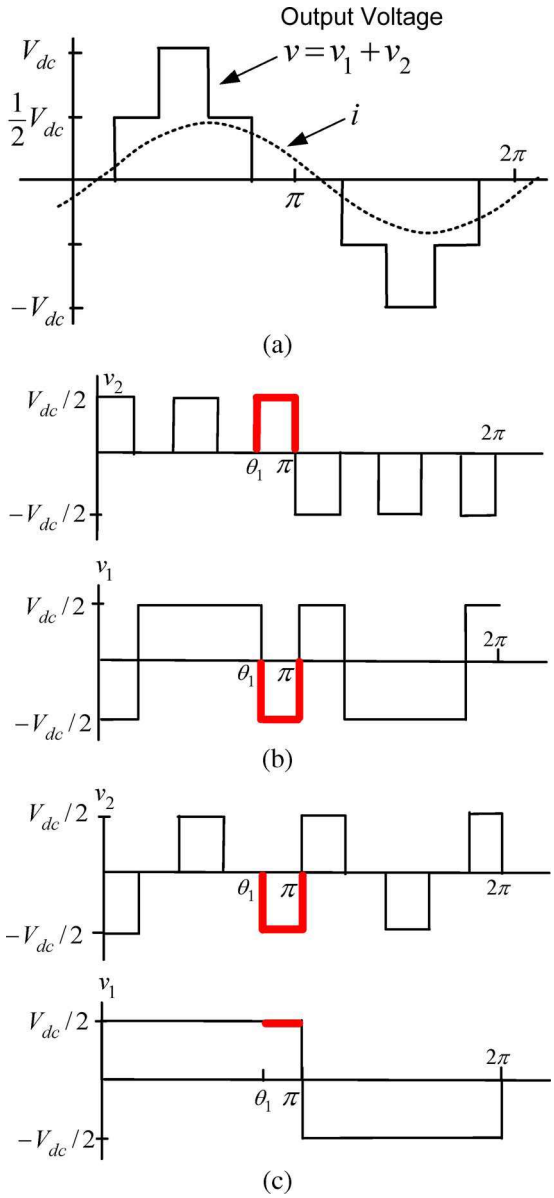

Fig. 3. Capacitor voltage regulation with capacitor charging and discharging. (a) Overall output voltage and load current. (b) Capacitor discharging. (c) Capacitor charging.

To see how the system works, a simplified single phase topology is shown in Fig. 2. The output voltage ν_1 of this leg of the bottom inverter (with respect to the ground) is either $+V_{\rm dc}/2$ (S_5 closed) or $-V_{\rm dc}/2$ (S_6 closed). This leg is connected in series with a full H-bridge, which, in turn, is supplied by a capacitor voltage. If the capacitor is kept charged to $V_{\rm dc}/2$, then the output voltage of the H-bridge can take on the values $+V_{\rm dc}/2$ (S_1 and S_4 closed), 0 (S_1 and S_2 closed or S_3 and S_4 closed), or $-V_{\rm dc}/2$ (S_2 and S_3 closed). An example output waveform from this topology is shown in Fig. 3(a). When the output voltage $\nu = \nu_1 + \nu_2$ is required to be zero, one can either set $\nu_1 = +V_{\rm dc}/2$ and $\nu_2 = -V_{\rm dc}/2$ or $\nu_1 = -V_{\rm dc}/2$ and $\nu_2 = +V_{\rm dc}/2$.

Additional capacitor's voltage regulation control detail is shown in Fig. 3. To explain how the capacitor is kept charged, consider the interval $\theta_1 \leq \theta \leq \pi$, the output voltage in Fig. 3(a) is zero, and the current $i > 0$. If S_1 and S_4 are closed (so that $\nu_2 = +V_{\rm dc}/2$) and S_6 is closed (so that $\nu_1 = -V_{\rm dc}/2$), then the capacitor is discharging [$i_c = -i < 0$; see Fig. 3(b)], and $\nu = \nu_1 + \nu_2 = 0$. On the other hand, if S_2 and S_3 are closed (so that $\nu_2 = -V_{\rm dc}/2$) and S_5 is also closed (so that $\nu_1 = +V_{\rm dc}/2$), then the capacitor is charging [$i_c = i > 0$; see Fig. 3(c)], and $\nu = \nu_1 + \nu_2 = 0$. The case $i < 0$ is accomplished by simply reversing the switch positions of the $i > 0$ case for charging and discharging of the capacitor. Consequently, the method consists of monitoring the output current and the capacitor voltage, so that during periods of zero voltage output, either the switches S_1, S_4, and S_6 are closed or the switches S_2, S_3, and S_5 are closed, depending on whether it is necessary to charge or discharge the capacitor. It is this flexibility in choosing how to make that output voltage zero that is exploited to regulate the capacitor voltage.

The goal of using fundamental frequency switching modulation control is to output a five-level voltage waveform, with a sinusoidal load current waveform, as shown in Fig. 3(a). If the capacitor's voltage is higher than $V_{\rm dc}/2$, switches S_5 and S_6

are controlled to output voltage waveform ν_1, and the switches S_1, S_2, S_3, and S_4 are controlled to output voltage waveform ν_2, shown in Fig. 3(b). The highlighted part of the waveform in Fig. 3(b) is the capacitor discharging period, during which the inverter's output voltage is 0 V.

If the capacitor's voltage is lower than $V_{\rm dc}/2$, the switches S_5 and S_6 are controlled to output voltage waveform ν_1, and switches S_1, S_2, S_3, and S_4 are controlled to output voltage waveform ν_2, shown in Fig. 3(c). The highlighted part of the waveform in Fig. 3(c) is the capacitor charging period, when the inverter's output voltage is 0 V. Therefore, the capacitors' voltage can be regulated by alternating the capacitor's charging and discharging control, when the inverter output is 0 V.

This method of regulating the capacitor voltage depends on the voltage and current not being in phase. That is, one needs positive (or negative) current when the voltage is passing through zero in order to charge or discharge the capacitor. Consequently, the amount of capacitor voltage the scheme can regulate depends on the phase angle difference of output voltage and current. In other words, the highest output ac voltage of the inverter depends on the displacement power factor of the load.

III. Switching Control of Cascaded H-Bridge Multilevel Boost Inverter Without Inductors

There are several kinds of modulation control methods such as traditional sinusoidal pulsewidth modulation (SPWM), [15]–[19], space vector PWM [20], harmonic optimization or selective harmonic elimination [21]–[28], and active harmonic elimination [29], and they all can be used for inverter modulation control. For the proposed dc–ac boost inverter control, a practical modulation control method is the fundamental frequency switching control for high output voltage and SPWM control for low output voltage, which only uses the bottom inverter. In this paper, the fundamental frequency switching control is used.

The Fourier series expansion of the fundamental frequency (staircase) output voltage waveform of the multilevel inverter, as shown in Fig. 3(a), is

$$V(\omega t)=\frac{4}{\pi}\frac{V_{\rm dc}}{2}\times\sum_{n=1,3,5,\ldots}^{\infty}\frac{1}{n}(\cos(n\theta_1)+\cos(n\theta_2))\sin(n\omega t). \tag{1}$$

The key issue of fundamental frequency modulation control is choice of the two switching angles θ_1 and θ_2. In this paper, the goal is to output the desired fundamental frequency voltage and to eliminate the fifth harmonic. Mathematically, this can be formulated as the solution to the following:

$$\begin{aligned}\cos(\theta_1)+\cos(\theta_2)&=m_a\\ \cos(5\theta_1)+\cos(5\theta_2)&=0.\end{aligned} \tag{2}$$

This is a system of two transcendental equations with two unknowns θ_1 and θ_2, and m_a is the output voltage index. Traditionally, the modulation index is defined as

$$m=\frac{V_1}{V_{\rm dc}/2}. \tag{3}$$

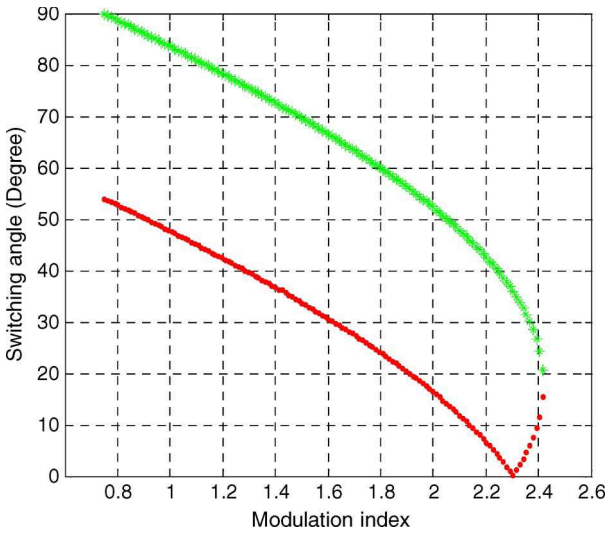

Fig. 4. Switching angle solutions for proposed dc–ac cascaded H-bridge multilevel boost inverter control.

Therefore, the relationship between the modulation index m and the output voltage index m_a is

$$m=\frac{4}{\pi}m_a. \tag{4}$$

There are many ways one can solve (2) for the angles. Here, the resultant method is used to find the switching angles. A practical solution set is shown in Fig. 4, which is continuous from modulation index 0.75 to 2.42 [26].

Although it can be seen from Fig. 4 that the modulation index range for the five-level fundamental frequency switching control method can reach 2.42, which is double that of the traditional power inverter, it requires the capacitors' voltage to be kept constant at $V_{\rm dc}/2$.

Traditionally, the maximum modulation index for the linear operation of a traditional full-bridge bilevel inverter using SPWM control method is 1 (without third harmonic compensation) and 1.15 (with third harmonic compensation, and the inverter output voltage waveform is an SPWM waveform, not a square waveform). With the cascaded H-bridge multilevel inverter, the maximum modulation index for linear operation can be as high as 2.42; however, the maximum modulation index depends on the displacement power factor, as will be shown in the next section.

IV. Output Voltage Boost

As previously mentioned, the cascaded H-bridge multilevel inverter can output a boosted ac voltage to increase the output power, and the output ac voltage depends on the displacement power factor of the load. Here, the relationship of the boosted ac voltage and the displacement power factor is discussed.

It is assumed that the load current displacement angle is φ, as shown in Fig. 5. To balance the capacitor voltage, the net capacitor charging amount needs to be greater than the pure discharging amount. That is, to regulate the capacitor's voltage

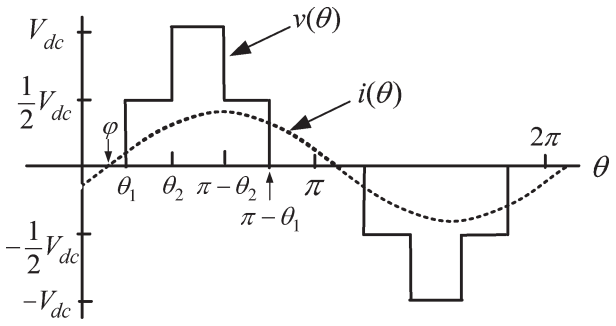

Fig. 5. Capacitor charging and discharging cases.

with a fundamental frequency switching scheme, the following must be satisfied:

$$\int_0^{\pi} i_{\text{charging}}\, d\theta - \int_0^{\pi} i_{\text{discharging}}\, d\theta > 0. \tag{5}$$

The charging and discharging of the current with an inductance load can be classified into three cases. The fundamental of the inductive load current is given by

$$i = I\sin(\omega t - \varphi) \tag{6}$$

and the displacement power factor is

$$pf = \cos(\varphi). \tag{7}$$

The three cases are as follows.

1) $0 \le \varphi \le \theta_1$

$$\int_0^{\varphi} |i|\, d\theta + \int_{\varphi}^{\theta_1} i\, d\theta + \int_{\pi-\theta_1}^{\pi} i\, d\theta - \int_{\theta_2}^{\pi-\theta_2} i\, d\theta > 0. \tag{8}$$

2) $\theta_1 < \varphi \le \theta_2$

$$\int_0^{\theta_1} |i|\, d\theta + \int_{\pi-\theta_1}^{\pi} i\, d\theta - \int_{\theta_2}^{\pi-\theta_2} i\, d\theta > 0. \tag{9}$$

3) $\theta_2 < \varphi \le \pi/2$

$$\int_0^{\theta_1} |i|\, d\theta + \int_{\pi-\theta_1}^{\pi} i\, d\theta - \int_{\theta_2}^{\pi-\theta_2} i\, d\theta > 0. \tag{10}$$

Combining (6)–(10), it can be concluded that, for $0 \le \varphi \le \theta_1$

$$pf \le \frac{\pi}{4m} \tag{11}$$

and, for $\theta_1 < \varphi \le \pi/2$.

$$pf \le \cos\left[\tan^{-1}\left(\frac{\cos(\theta_2)}{\sin(\theta_1)}\right)\right]. \tag{12}$$

Therefore, the conditions for the fundamental frequency switching scheme to eliminate the fifth harmonic and to regulate the capacitor's voltage are (11) and (12).

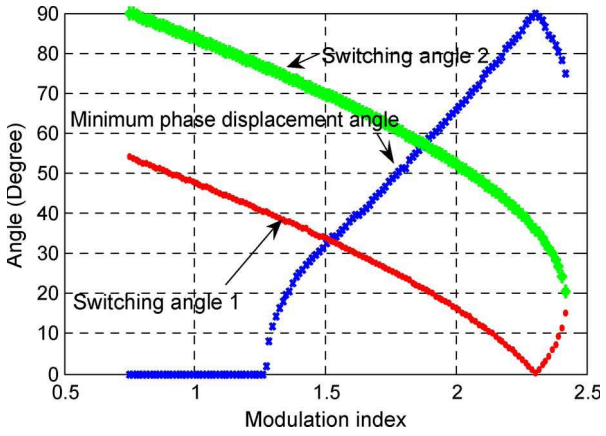

Fig. 6. Minimum phase displacement angle.

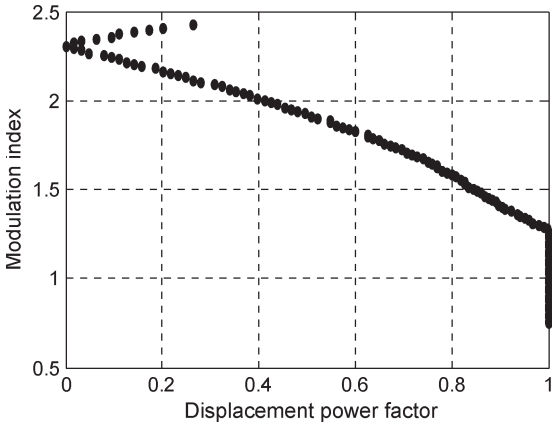

Fig. 7. Displacement power factor and output voltage modulation index.

For practical applications, direct use of (11) and (12) is not convenient. Using minimum phase displacement angles is a more convenient way to use (11) and (12). That means that, if the phase displacement angle is greater than the minimum angle, the voltage can be regulated anyway.

Fig. 6 shows the minimum phase displacement angle computed by (5)–(12). From the figure, it can be seen that, for modulation index range $m < 1.27$ (the inverter output is a five-level waveform, not a bilevel or square waveform), the minimum phase angle displacement is zero, which means that the capacitor's voltage can be regulated for all displacement power factors in this modulation index range. For modulation index range $m > 1.27$, the required minimum phase displacement angle is shown in Fig. 6. Fig. 6 also shows the two switching angles.

The phase displacement power factor versus the output voltage modulation index is shown in Fig. 7.

It can be derived from Fig. 7 that the highest output voltage modulation index depends on the displacement power factor. The inverter can regulate the capacitor's voltage with a displacement power factor of one if the modulation index is below 1.27; if the modulation index is above 1.27, the displacement power factor must be less than a specified amount. For practical applications, the highest output voltage is determined when the load is determined.

As mentioned previously, there are many methods to do modulation control for the proposed dc–ac cascaded H-bridge multilevel boost inverter without inductors. The fundamental

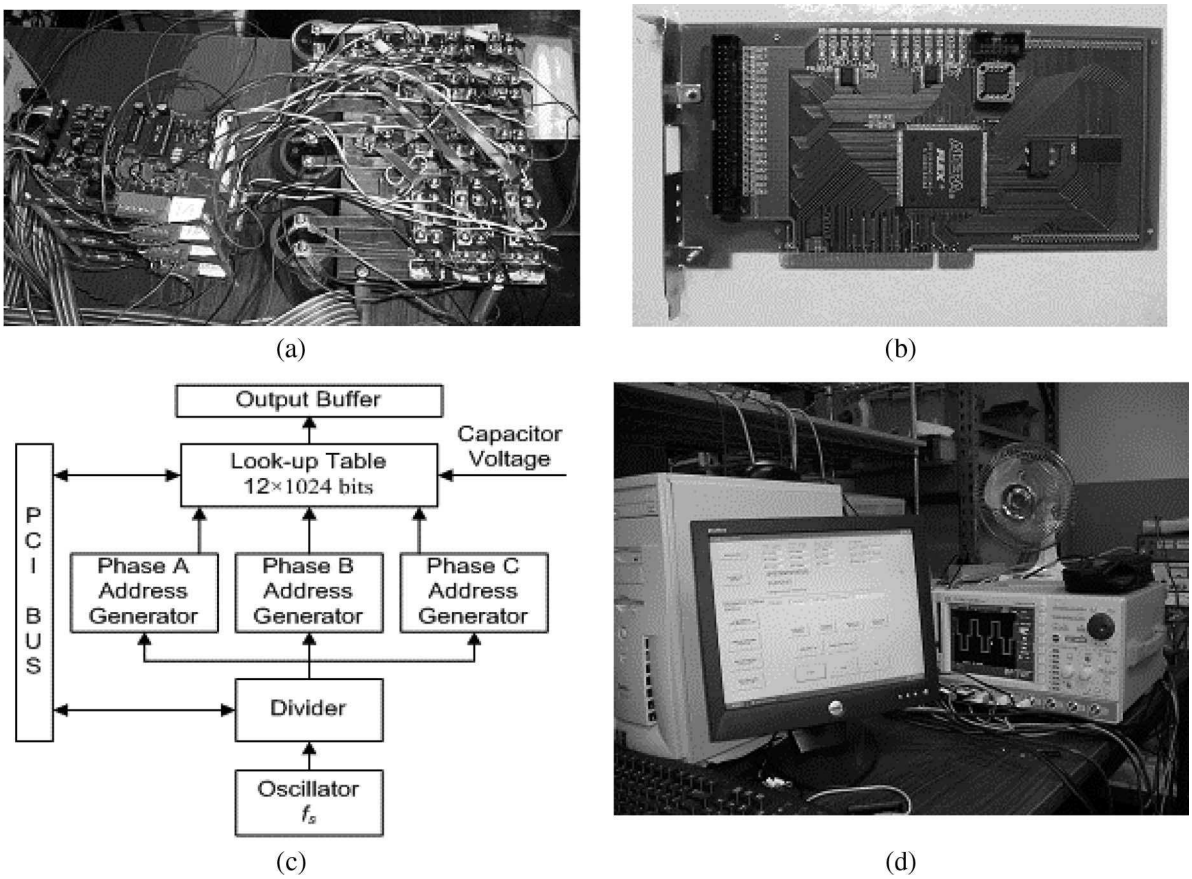

Fig. 8. (a) Five-kilowatt dc–ac cascaded H-bridge multilevel boost inverter prototype. (b) FPGA controller. (c) Block diagram of FPGA controller. (d) Bench setup.

frequency method with regulated $V_{\rm dc}/2$ capacitor voltage is only one of the possible methods to output continuous power. The traditional SPWM method can also be applied to this inverter to boost the output voltage with a lower maximum continuous output power and high switching loss but better THD for a lower output frequency range. It is also possible to use SPWM for low output frequency low output voltage conditions and staircase waveform for high output frequency high output voltage range to achieve optimal performances with maximum continuous output power, lower switching loss, and lower THD. It can also be seen that accurate load inductance is not required for controller design, and the controller is robust independent of the leakage inductance of stator windings. For HEV and EV applications, sometimes, only short period peak power is required. The modulation control can store energy to the capacitors by boosting the capacitor voltage to a higher voltage, which could be higher than $V_{\rm dc}$ when the vehicle is working in a low power mode. When the vehicle is working in high power modes, the capacitors will deliver much higher power than the continuous power to the motor load combined with the battery, fuel cell, or generator. This feature will greatly improve the vehicle's dynamic (acceleration) performance.

V. Experimental Implementation and Validation

To experimentally validate the proposed control scheme, a prototype 5-kW three-phase cascaded H-bridge multilevel converter has been built using 100-V 180-A MOSFETs as the switching devices [shown in Fig. 8(a)]. A real-time variable-output-voltage variable-frequency three-phase motor drive controller based on an Altera FLEX 10 K field programmable gate array (FPGA) is used to implement the control algorithm. For convenience of operation, the FPGA controller is designed as a card to be plugged into a personal computer, shown in Fig. 8(b), which uses a peripheral component interconnect bus to communicate with the microcomputer. To maintain the capacitors' voltage balance, a voltage sensor is used to detect the capacitors' voltage and feed the voltage signal into the FPGA controller. The FPGA controller will output the corresponding switching signals according to the capacitor's voltage. A 15-hp induction motor was used to load the inverter, and the motor was loaded to less than 5 kW in the experiments. The block diagram of the FPGA controller is shown in Fig. 8(c). The whole bench setup is shown in Fig. 8(d).

The switching signal data are stored in a 12 $\times$ 1024-b on-chip RAM. An oscillator generates a fixed frequency clock signal, and a divider is used to generate the specified control clock signal corresponding to the converter output frequency. Three-phase address generators share a public switching data RAM because they have the same switching data with only a different phase angle. (Because the switching data are symmetric, the switching data are only for one half cycle.) For each step, the three-phase signal controller controls the address selector to fetch the corresponding switching data from

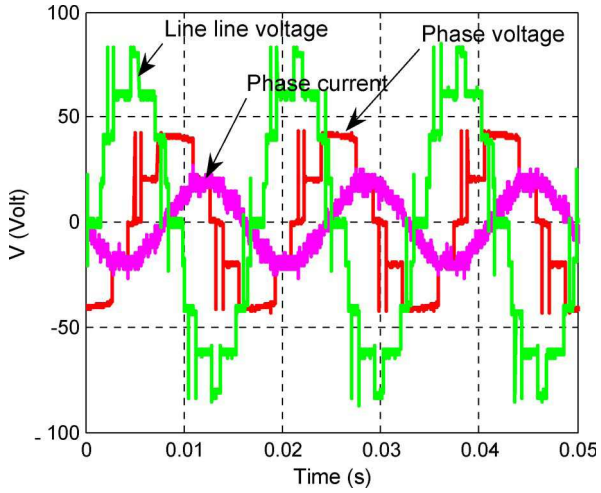

Fig. 9. Phase voltage waveform, line–line voltage waveform, and current waveform with 15-hp induction motor load ($m = 2.03$, and $f = 60$ Hz).

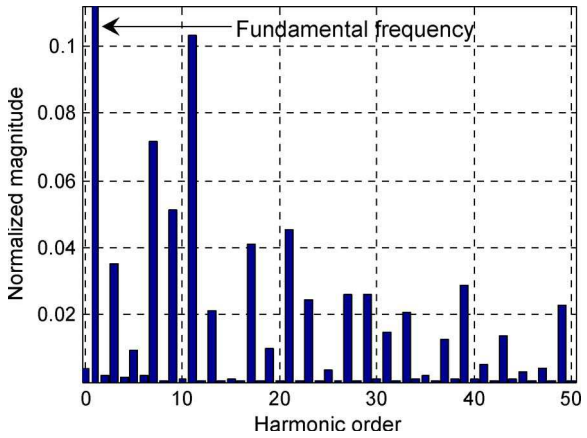

Fig. 10. Normalized FFT analysis of phase voltage.

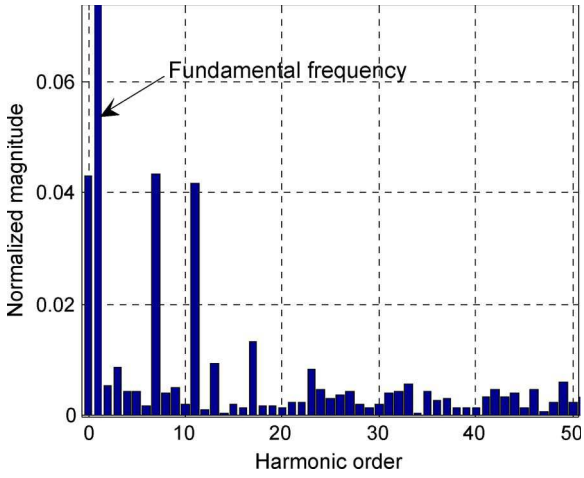

Fig. 11. Normalized FFT analysis of phase current.

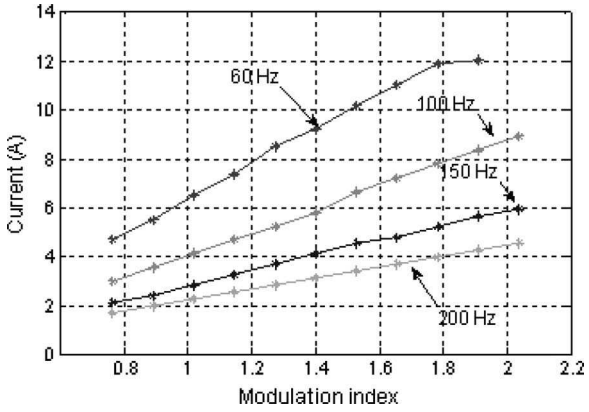

Fig. 12. Load current versus modulation index with different fundamental frequencies.

the RAM to the output buffer according to the capacitor's voltage.

Fig. 9 shows the output phase voltage waveform, line–line voltage waveform, and phase current waveform with an output frequency of 60 Hz. The modulation index of the output voltage is 2.03, and the capacitors' voltage is regulated to $V_{\rm dc}/2$. The phase voltage waveform shows that the output voltage has five levels, the line–line voltage has nine levels, and the phase current is a near-sinusoidal waveform.

Fig. 10 shows the normalized fast Fourier transform (FFT) analysis of the phase voltage, and that the fifth harmonic is very low (below 1%). Fig. 11 shows the normalized FFT analysis of the phase current, which also has a very low fifth harmonic content of 0.3%.

The experimental results and their FFT analysis all verified the performance of the fundamental frequency switching control. The modulation index in this experiment is from 0 to 2.03, which is much wider than the normal modulation index range 0–1.15 for traditional standard three-leg inverters.

To further test the cascaded multilevel boost inverter, experiments with load current versus modulation indexes with different fundamental frequencies were performed to achieve the highest output voltages. These were implemented by using an R–L load bank and compared to a traditional inverter.

For these experiments, the R–L load was fixed, the modulation index was changed with different fundamental frequencies, and the load currents were recorded. The load current curves for frequencies 60, 100, 150, and 200 Hz are shown in Fig. 12.

Fig. 12 shows that, in the working range of the cascaded multilevel boost inverter without inductors, the load current and the modulation index are linear. This feature is similar to the traditional inverter and allows easy implementation for practical applications.

In this experiment, to achieve the highest output voltages for the cascaded multilevel boost inverter without inductors and the traditional inverter, two steps were involved. First, the load was connected to the bottom traditional inverter to output its highest voltage; second, the load was connected to the cascaded H-bridge multilevel inverter with the same dc power supply voltage. The output voltages for the two cases are shown in Table I.

Table I shows that the highest output voltage of the cascaded H-bridge multilevel inverter is much higher than that of the traditional inverter. The voltage boost ratio is higher than 1.4 for the whole testing frequency range.

TABLE I
HIGHEST OUTPUT VOLTAGE FOR TRADITIONAL INVERTER AND CASCADED H-BRIDGE MULTILEVEL INVERTER (DC BUS IS 40 V)

Test frequency (Hz)	Traditional inverter output voltage (V)	Cascaded H-bridge multilevel inverter output voltage (V)	Boost ratio
200	23.1	42.8	1.85
150	23.1	42.2	1.82
100	23.1	41.2	1.78
60	23.1	37.7	1.63
40	23.1	33.1	1.43

Table I also shows that the highest output voltage of the inverter is decreasing when the frequency is decreasing; this is because the impedance of the inductor is decreasing. Another issue is that the boost voltage ratio is decreasing when the frequency is decreasing; this is because the power factor is increasing for the fixed R–L load.

VI. CONCLUSION

The proposed cascaded H-bridge multilevel boost inverter without inductors uses a standard three-leg inverter (one leg for each phase) and an H-bridge in series with each inverter leg. A fundamental switching scheme is used for modulation control, to output five-level phase voltages. Experiments show that the proposed dc–ac cascaded H-bridge multilevel boost inverter can output a boosted ac voltage with the same dc power supply, which has a wider modulation index range than a traditional inverter. The application of this dc–ac boost inverter on HEV and EV can result in the elimination of the bulky inductor of present dc–dc boost converters, thereby increasing the power density.

ACKNOWLEDGMENT

This paper has been authored by a contractor of the U.S. Government under Contract DE-AC05-00OR22725. Accordingly, the U.S. Government retains a nonexclusive royalty-free license to publish from the contribution, or allow others to do so, for U.S. Government purposes.

REFERENCES

[1] K. M. Rahman, N. R. Patel, T. G. Ward, J. M. Nagashima, F. Caricchi, and F. Crescimbini, "Application of direct-drive wheel motor for fuel cell electric and hybrid electric vehicle propulsion system," *IEEE Trans. Ind. Appl.*, vol. 42, no. 5, pp. 1185–1192, Sep./Oct. 2006.

[2] M. Hinkkanen and J. Luomi, "Braking scheme for vector-controlled induction motor drives equipped with diode rectifier without braking resistor," *IEEE Trans. Ind. Appl.*, vol. 42, no. 5, pp. 1257–1263, Sep./Oct. 2006.

[3] C. H. Rivetta, A. Emadi, G. A. Williamson, R. Jayabalan, and B. Fahimi, "Analysis and control of a buck dc–dc converter operating with constant power load in sea and undersea vehicles," *IEEE Trans. Ind. Appl.*, vol. 42, no. 2, pp. 559–572, Mar./Apr. 2006.

[4] J. S. Lai and F. Z. Peng, "Multilevel converters—A new breed of power converters," *IEEE Trans. Ind. Appl.*, vol. 32, no. 3, pp. 36–44, May/Jun. 1996.

[5] J. S. Lai, J. Rodriguez, J. Lai, and F. Peng, "Multilevel inverters: A survey of topologies, controls and applications," *IEEE Trans. Ind. Appl.*, vol. 49, no. 4, pp. 724–738, Aug. 2002.

[6] L. M. Tolbert, F. Z. Peng, and T. G. Habetler, "Multilevel converters for large electric drives," *IEEE Trans. Ind. Appl.*, vol. 35, no. 1, pp. 36–44, Jan./Feb. 1999.

[7] C. B. Jacobina, E. C. dos Santos, M. B. de Rossiter Correa, and E. R. C. da Silva, "AC motor drives with a reduced number of switches and boost inductors," *IEEE Trans. Ind. Appl.*, vol. 43, no. 1, pp. 30–39, Jan./Feb. 2007.

[8] L. Ben-Brahim and S. Tadakuma, "A novel multilevel carrier-based PWM-control method for GTO inverter in low index modulation region," *IEEE Trans. Ind. Appl.*, vol. 42, no. 1, pp. 121–127, Jan./Feb. 2006.

[9] L. Schuch, C. Rech, H. L. Hey, H. A. Grundling, H. Pinheiro, and J. R. Pinheiro, "Analysis and design of a new high-efficiency bidirectional integrated ZVT PWM converter for dc-bus and battery-bank interface," *IEEE Trans. Ind. Appl.*, vol. 42, no. 5, pp. 1321–1332, Sep./Oct. 2006.

[10] M. Shen, J. Wang, A. Joseph, F. Z. Peng, L. M. Tolbert, and D. J. Adams, "Constant boost control of the Z-source inverter to minimize current ripple and voltage stress," *IEEE Trans. Ind. Appl.*, vol. 42, no. 3, pp. 770–778, May/Jun. 2006.

[11] Z. Du, L. M. Tolbert, and J. N. Chiasson, "A cascade multilevel inverter using a single DC source," in *Conf. Rec. IEEE APEC*, Dallas, TX, 2006, pp. 426–430.

[12] K. A. Corzine, F. A. Hardrick, and Y. L. Familiant, "A cascaded multilevel H-bridge inverter utilizing capacitor voltages sources," in *Proc. IASTED Conf.-PES*, Palm Springs, CA, 2003, pp. 290–295.

[13] J. N. Chiasson, B. Özpineci, and L. M. Tolbert, "Five-level three-phase hybrid cascade multilevel inverter using a single dc source," in *Conf. Rec. IEEE APEC*, Anaheim, CA, 2007, pp. 1504–1507.

[14] J. N. Chiasson, B. Özpineci, Z. Du, and L. M. Tolbert, "Conditions for capacitor voltage regulation in a five-level cascade multilevel inverter: Application to voltage-boost in a PM drive," in *Conf. Rec. IEEE IEMDC*. Antalya, Turkey, 2007, pp. 731–735.

[15] J. K. Steinke, "Control strategy for a three phase AC traction drive with a 3-level GTO PWM inverter," in *Conf. Rec. IEEE PESC*, 1988, pp. 431–438.

[16] P. Hammond, "A new approach to enhance power quality for medium voltage ac drives," *IEEE Trans. Ind. Appl.*, vol. 33, no. 1, pp. 202–208, Jan./Feb. 1997.

[17] W. A. Hill and C. D. Harbourt, "Performance of medium voltage multilevel inverters," in *Conf. Rec. IEEE IAS Annu. Meeting*, Phoenix, AZ, 1999, pp. 1186–1192.

[18] G. Carrara, S. Gardella, M. Marchesoni, R. Salutari, and G. Sciutto, "A new multilevel PWM method: A theoretical analysis," *IEEE Trans. Power Electron.*, vol. 7, no. 3, pp. 497–505, Jul. 1992.

[19] L. M. Tolbert, F. Z. Peng, and T. G. Habetler, "Multilevel PWM methods at low modulation indices," *IEEE Trans. Power Electron.*, vol. 15, no. 4, pp. 719–725, Jul. 2000.

[20] D. G. Holmes, "The significance of zero space vector placement for carrier based PWM schemes," in *Conf. Rec. IEEE IAS Annu. Meeting*, 1995, pp. 2451–2458.

[21] J. Vassallo, J. C. Clare, and P. W. Wheeler, "A power-equalized harmonic-elimination scheme for utility-connected cascaded H-bridge multilevel converters," in *Conf. Rec. IEEE IES*, 2003, pp. 1185–1190.

[22] S. Sirisukprasert, J.-S. Lai, and T.-H. Liu, "Optimum harmonic reduction with a wide range of modulation indexes for multilevel converters," *IEEE Trans. Ind. Electron.*, vol. 49, no. 4, pp. 875–881, Aug. 2002.

[23] P. C. Loh, D. G. Holmes, and T. A. Lipo, "Implementation and control of distributed PWM cascaded multilevel inverters with minimum harmonic distortion and common-mode voltages," *IEEE Trans. Power Electron.*, vol. 20, no. 1, pp. 90–99, Jan. 2005.

[24] H. S. Patel and R. G. Hoft, "Generalized harmonic elimination and voltage control in thyristor inverters: Part I—Harmonic elimination," *IEEE Trans. Ind. Appl.*, vol. IA-9, no. 3, pp. 310–317, May/Jun. 1973.

[25] H. S. Patel and R. G. Hoft, "Generalized harmonic elimination and voltage control in thyristor inverters: Part II—Voltage control technique," *IEEE Trans. Ind. Appl.*, vol. IA-10, no. 5, pp. 666–673, Sep./Oct. 1974.

[26] J. N. Chiasson, L. M. Tolbert, K. J. McKenzie, and Z. Du, "Control of a multilevel converter using resultant theory," *IEEE Trans. Control Syst. Technol.*, vol. 11, no. 3, pp. 345–354, May 2003.

[27] P. N. Enjeti, P. D. Ziogas, and J. F. Lindsay, "Programmed PWM techniques to eliminate harmonics: A critical evaluation," *IEEE Trans. Ind. Appl.*, vol. 26, no. 2, pp. 302–316, Mar./Apr. 1990.

[28] T. Kato, "Sequential homotopy-based computation of multiple solutions for selected harmonic elimination in PWM inverters," *IEEE Trans. Circuits Syst. I, Fundam. Theory Appl.*, vol. 46, no. 5, pp. 586–593, May 1999.

[29] Z. Du, L. M. Tolbert, and J. N. Chiasson, "Active harmonic elimination for multilevel converters," *IEEE Trans. Power Electron.*, vol. 21, no. 2, pp. 459–469, Mar. 2006.

Zhong Du (S'01–M'05) received the B.S. degree in process automation instrumentation and the M.S. degree in power machinery and engineering from Tsinghua University, Beijing, China, in 1996 and 1999, respectively, and the Ph.D. degree in electrical engineering from The University of Tennessee, Knoxville, in 2005.

He was a Research Associate with the National Transportation Research Center, Oak Ridge National Laboratory, Oak Ridge, TN. He was a Research Assistant Professor with North Carolina State University, Raleigh. Since 2007, he has been with Parker Hannifin Corporation, Olive Branch, MS, where he is working on hybrid diesel trucks. He has been conducting research and development on hybrid vehicles, utility power electronics systems, and distributed energy systems.

Burak Ozpineci (S'92–M'02–SM'05) received the B.S. degree in electrical engineering from the Middle East Technical University, Ankara, Turkey, in 1994, and the M.S. and Ph.D. degrees in electrical engineering from The University of Tennessee, Knoxville, in 1998 and 2002, respectively.

In 2001, he joined the Postmasters Program with the Power Electronics and Electric Machinery Research Center, Oak Ridge National Laboratory (ORNL), Knoxville, where he became a Full Time Research and Development Staff Member in 2002 and has been a Technical Program Manager since 2006. He also has an Adjunct Faculty appointment with the University of Arkansas, Fayetteville. He is conducting research on the system-level impact of SiC power devices, multilevel inverters, power converters for distributed energy resources and hybrid electric vehicles, and intelligent control applications for power converters.

Dr. Ozpineci was the Chair of the IEEE Power Electronics Society Rectifiers and Inverters Technical Committee and the TRANSACTIONS Review Chairman of the IEEE Industry Applications Society Industrial Power Converter Committee. He was the recipient of the 2006 IEEE Industry Applications Society Outstanding Young Member Award; the 2001 IEEE International Conference on Systems, Man, and Cybernetics Best Student Paper Award; and the 2005 UT-Battelle (ORNL) Early Career Award for Engineering Accomplishment.

Leon M. Tolbert (S'89–M'91–SM'98) received the B.E.E., M.S., and Ph.D. degrees in electrical engineering from Georgia Institute of Technology, Atlanta, in 1989, 1991, and 1999, respectively.

In 1991, he was with the Engineering Division, Lockheed Martin Energy Systems, where he worked on several electrical distribution projects at the three U.S. Department of Energy plants in Oak Ridge, TN. In 1997, he was a Research Engineer with the Power Electronics and Electric Machinery Research Center, Oak Ridge National Laboratory (ORNL), Oak Ridge. Since 1999, he has been with the Department of Electrical and Computer Engineering, The University of Tennessee, Knoxville, where he is currently an Associate Professor. He is also an Adjunct Participant with ORNL and conducts joint research with the National Transportation Research Center. He conducts research in the areas of electric power conversion for distributed energy sources, motor drives, multilevel converters, hybrid electric vehicles, and application of SiC power electronics.

Dr. Tolbert is a Registered Professional Engineer in the State of Tennessee. He was the Coordinator of Special Activities for the Industrial Power Converter Committee of the IEEE Industry Applications Society (IAS), from 2003 to 2006. He was the Chair of the Educational Activities Committee of the IEEE Power Electronics Society from 2003 to 2007. He was an Associate Editor of the IEEE POWER ELECTRONICS LETTERS from 2003 to 2006. He is an Associate Editor of the IEEE TRANSACTIONS ON POWER ELECTRONICS. He was the recipient of the 2001 IAS Outstanding Young Member Award.

John N. Chiasson (S'82–M'84–SM'03) received the B.S. degree in mathematics from the University of Arizona, Tucson, the M.S. degree in electrical engineering from Washington State University, Pullman, and the Ph.D. degree in controls from the University of Minnesota, Minneapolis.

He has worked in industry with Boeing Aerospace, Control Data, and ABB Daimler-Benz Transportation. He is currently an Associate Professor of electrical and computer engineering at Boise State University, Boise, ID. He is the author of the recent textbook *Modeling and High-Performance Control of Electric Machines* (Wiley 2005). His research interests include control of ac electric drives and multilevel converters.